Hindawi
Journal of Nanomaterials
Volume 2023, Article ID 9851384, 1 page
https://doi.org/10.1155/2023/9851384

Retraction

Retracted: Meta-Analysis of the Main Components of Nanophotodynamics Combined with Traditional Chinese Medicine in the Treatment of Tumors

Journal of Nanomaterials

Received 18 July 2023; Accepted 18 July 2023; Published 19 July 2023

This article has been retracted by Hindawi following an investigation undertaken by the publisher [1]. This investigation has uncovered evidence of one or more of the following indicators of systematic manipulation of the publication process:

(1) Discrepancies in scope
(2) Discrepancies in the description of the research reported
(3) Discrepancies between the availability of data and the research described
(4) Inappropriate citations
(5) Incoherent, meaningless and/or irrelevant content included in the article
(6) Peer-review manipulation

The presence of these indicators undermines our confidence in the integrity of the article's content and we cannot, therefore, vouch for its reliability. Please note that this notice is intended solely to alert readers that the content of this article is unreliable. We have not investigated whether authors were aware of or involved in the systematic manipulation of the publication process.

Wiley and Hindawi regrets that the usual quality checks did not identify these issues before publication and have since put additional measures in place to safeguard research integrity.

We wish to credit our own Research Integrity and Research Publishing teams and anonymous and named external researchers and research integrity experts for contributing to this investigation.

The corresponding author, as the representative of all authors, has been given the opportunity to register their agreement or disagreement to this retraction. We have kept a record of any response received.

References

[1] Y. Liu, Y. Li, and Y. Wen, "Meta-Analysis of the Main Components of Nanophotodynamics Combined with Traditional Chinese Medicine in the Treatment of Tumors," *Journal of Nanomaterials*, vol. 2022, Article ID 4552356, 14 pages, 2022.

Hindawi
Journal of Nanomaterials
Volume 2022, Article ID 4552356, 14 pages
https://doi.org/10.1155/2022/4552356

Research Article

Meta-Analysis of the Main Components of Nanophotodynamics Combined with Traditional Chinese Medicine in the Treatment of Tumors

Ying Liu,[1] Yanwei Li,[1] and Yulong Wen[2]

[1]*Clinical Medical College/Affiliated Hospital, Chengdu University of Traditional Chinese Medicine, Chengdu, 610032 Sichuan, China*
[2]*School of Basic Medical Sciences, Chengdu University of Traditional Chinese Medicine, Chengdu, 611137 Sichuan, China*

Correspondence should be addressed to Yulong Wen; wenyulong@cdutcm.edu.cn

Received 22 March 2022; Revised 28 April 2022; Accepted 11 May 2022; Published 8 June 2022

Academic Editor: Awais Ahmed

At present, cancer has become one of the main reasons that affect people's life and health. With the development of nanomaterials and nanotechnology, tumor phototherapy such as photodynamic therapy, photothermal therapy, and combination therapy has been developed rapidly. Based on this, this paper proposes to take gastric cancer, esophageal cancer, liver cancer, intestinal cancer, and pancreatic cancer as the starting point and apply the methods of network meta-analysis to comprehensively carry out the horizontal comprehensive evaluation of the efficacy and safety of traditional Chinese medicine injections. It is hoped that this article can provide high-quality evidence-based medicine for clinical decision-making and promote clinical rational drug use. The purpose of this paper is to study the meta-analysis of the main components of tumor treatment with nanophotodynamics combined with traditional Chinese medicine. The experimental results in this paper show that non-small-cell lung cancer has the largest number of evaluations, with 77 evaluations, accounting for 38.5% of the total frequency of tumor types. This may be related to the fact that lung cancer ranks first in the morbidity and mortality of malignant tumors. It is followed by the evaluation times of liver cancer and gastric cancer, which were 29 times and 25 times, respectively, accounting for 14.5% and 12.5% of the total frequency of tumor types. The therapeutic effect of SM-NP light therapy group on tumor was significantly higher than that of free Ce6 light therapy group, and its destruction and killing effect on tumor tissue was greater.

1. Introduction

The high recurrence rate, easy spread, and poor prognosis of tumors are the main challenges of clinical treatment. Currently, surgery, chemotherapy, and radiotherapy are the three main methods of clinical treatment of cancer. It has been widely used in tumor therapy, but it is difficult to inhibit it. It is effective in the treatment of malignant tumors. An ideal therapeutic strategy can not only effectively and safely remove tumors in situ but also prevent tumor metastasis by activating the body's immune system to recognize and remove tumor cells.

Chemotherapy is one of the important methods for the treatment of malignant tumors. However, traditional chemotherapeutic drugs lack tumor selectivity and have serious side effects. Photodynamic therapy is a new cancer treatment method developed in recent years. Photosensitive drugs enter the body and accumulate under the concentration and generate singlet active oxygen under the action of laser light of absorption wavelength, thereby producing cytotoxic effect. As a safe and efficient cancer treatment, photodynamic therapy can not only directly kill tumor cells but also potentially improve the immunogenicity of tumor cells. It induces an antitumor immune effect and meets the clinical demand for combined tumor therapy.

The innovation of this paper is to explore new research methods to comprehensively evaluate the efficacy and safety of different types of traditional Chinese medicine injections in the treatment of digestive system tumors, which has important academic significance and clinical value. This paper evaluates the antitumor efficacy and biosafety of photodynamic nanodrugs by analyzing the data, which is the basis for clinical tumor treatment application method and data reference.

2. Related Work

In recent years, photodynamic therapy (PDT) has become a research hotspot in the field of tumor therapy due to its noninvasive and spatiotemporal controllable advantages. Synergistic therapy and precise drug delivery at the tumor site have emerged as a promising strategy to achieve tumor eradication. Here, Li et al. prepare smart near-infrared fluorescence imaging-guided nanoliposomes L@CY@DOX by encapsulating a chemotherapeutic drug (doxorubicin), liposome (L), and a near-infrared (NIR) photosensitizer (CY). It can enhance the therapeutic effect of chemotherapeutic PDT in cancer treatment [1]. Lack of selectivity of tumor cells and overproduction of glutathione (GSH) are two major challenges for efficient and safe cancer PDT, because they cause damage to normal tissues and scavenge ROS in cancer cells. Herein, Pan et al. report a GSH-responsive nanophotosensitizer based on CoOOH nanosheets for PDT of cancer. The current nanophotosensitizers represent a promising smart platform to synergistically improve the therapeutic index and safety of PDT [2]. Recently developed photodynamic therapy has received much attention for achieving effective root canal disinfection. It uses an optimized nontoxic photosensitizer (PS) such as indocyanine green (ICG). It is an integral part of this technology. Therefore, the aim of Akbari et al.'s study was to improve the photodynamic properties of ICG by incorporating ICG into nanographene oxide (NGO). It prepared NGO-ICG as a new PS and evaluated the antibacterial effect of NGO-ICG on Enterococcus faecalis after photodynamic therapy [3]. The application of traditional photodynamic therapy (PDT) is often limited by insufficient oxygen supply, and it is difficult to achieve high PDT efficacy. Herein, Qin et al. combine liposomes with photosensitizers indocyanine green (ICG) and perfluorooctyl bromide (PFOB) to develop a novel oxygen-enriched photodynamic nanospray for postoperative cancer therapy. This oxygen-enriched photodynamic nanospray strategy may open new avenues for clinically effective postoperative cancer therapy [4]. Photoimmunotherapy is a new treatment approach that is minimally invasive for malignant tumors. Here, Zhang et al. designed a targeted multifunctional black phosphorus (BP) nanoparticle, modified with PEGylated hyaluronic acid (HA) for photothermal/photodynamic/photoimmunotherapy. In vitro and in vivo experiments demonstrated that HA-BP nanoparticles have good biocompatibility, stability, and sufficient efficacy in the combined photothermal therapy (PTT) and photodynamic therapy (PDT) treatment of cancer. Zhang et al.'s research expands the biomedical applications of BP nanoparticles, demonstrating the potential of modified BP as a multifunctional therapeutic platform for future cancer treatment [5]. Wang et al. design a versatile and powerful nanoplatform. They have cleverly integrated multiple molecules with therapeutic and diagnostic properties to stimulate the delivery of responsive drugs to lesions. This is still a huge challenge. Here, Wang et al. report a facile and ingenious cross-linked nanogel based on medicinal chemical cross-linking as a straightforward strategy to overcome assembly instability. This work provides a unique strategy for designing a series of prodrug nanogels as a universal drug delivery platform for precise disease therapy and diagnosis [6]. Deng et al. developed the mitochondria-targeted biodegradable polymer polylactic acid. The data suggest that X-PDT treatment has cytoreductive, antiproliferative, and profibrotic effects. The nanocarriers effectively enhance the radiosensitization effect, which makes it possible to enhance the radiation effect [7]. Lack of selectivity of tumor cells and overproduction of glutathione (GSH) are two major challenges for efficient and safe cancer PDT because they cause damage to normal tissues and scavenge ROS in cancer cells. Herein, Wei et al. reported a GSH-responsive nanophotosensitizer based on CoOOH nanosheets for PDT of cancer [2]. However, the shortcomings of these studies are that the model construction is not scientific enough and the data is limited to adapt to more complex situations.

3. Nanophotodynamic Therapy-Related Methods of Tumor

3.1. Advantages and Development Status of Photodynamic Therapy for Cancer

3.1.1. Photodynamic Therapy. Over the past few decades, photodynamic therapy (PDT) has undergone tremendous progress as a treatment modality. It includes age-related macular degeneration, psoriasis, atherosclerosis, and various malignancies. It mainly activates the photosensitizer (PS) accumulated at the tumor site by light with a specific wavelength. The activated PS transfers energy to surrounding oxygen molecules, resulting in the reduction of oxygen and the generation of reactive oxygen species (ROS) (Figure 1). Oxidation of biomacromolecules results in tumor reduction, vascular damage, local acute inflammation, and immune responses [8].

Compared with traditional treatment methods, PDT is due to its weak invasiveness, ideal convenience and flexibility, effective curative effect, and high patient acceptance. It has laid a solid foundation for the clinical application of PDT. Since the advent of the first approved PDT prodrug procarbazine in 1970, three photosensitizers, protoporphyrin, verteporfin, and 5-aminolevulinic acid, have been approved by the FDA. More than 16 drugs have subsequently entered clinical trials or are on the market. Compared with traditional treatments, PDT still has many limitations as a first-line clinical treatment due to the lack of effective photosensitizers, appropriate light doses, and effective photosensitizer delivery [9].

In drug delivery systems, light is a common external stimulus used to trigger drug release. Compared with complex and uncontrollable internal stimuli, light can control drug release in a more controllable time and space. Based on the process of PDT oxygen consumption and ROS generation, PDT can be combined with nanomedicines sensitive

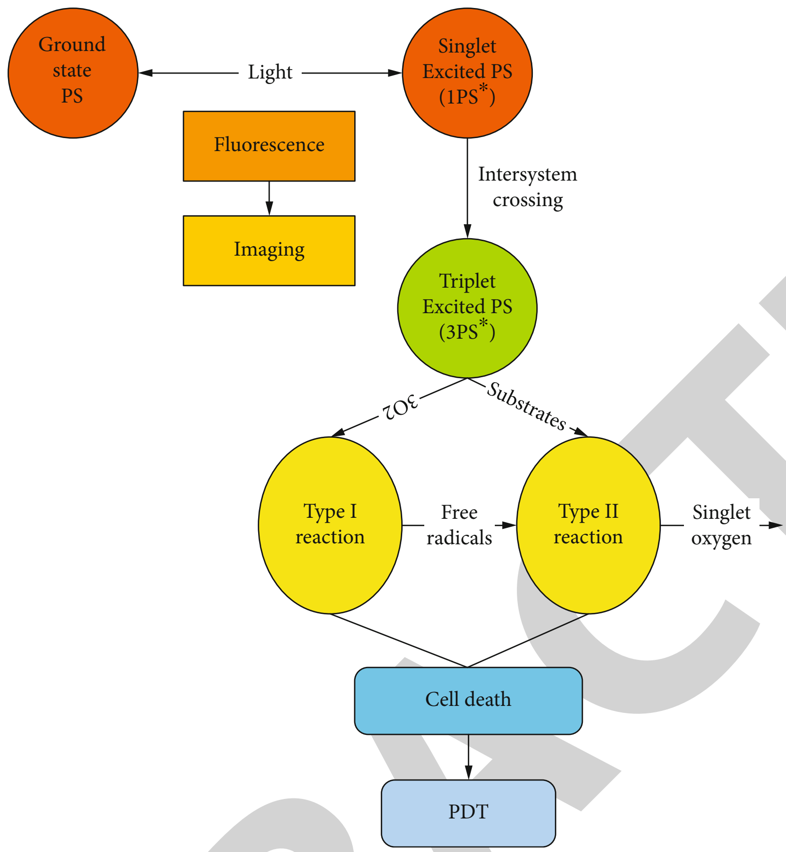

Figure 1: Schematic diagram of a typical photodynamic reaction.

to the tumor microenvironment (such as ROS, hypoxia), and finally, it achieves a positive feedback and synergistic treatment effect [10].

3.1.2. Advantages of Photodynamic Therapy for Cancer. Photosensitizers, excitation light, and oxygen molecules are three important elements for PDT. The mechanism of action of photodynamic therapy is to utilize the selective enrichment of photosensitizers in tumor tissue. It converts oxygen into reactive oxygen species (ROS) that can kill cells through a laser-triggered photosensitizer with strong tissue penetration. It can oxidatively damage surrounding organelles and biomolecules, eventually inducing tumor cell necrosis and apoptosis, sealing tumor blood vessels, and causing vascular damage [11]. In addition, photodynamic therapy is often accompanied by the production of acute inflammation. Through the recruitment and activation of immune cells such as neutrophils and dendritic cells at the tumor site, acute inflammation in the local tumor is triggered, and an immune response is generated to further kill the tumor.

3.1.3. Tumor Phototherapy. In recent years, cancer, namely, malignant tumor, has become one of the important diseases threatening human health worldwide, although human beings have deeply researched on the mechanism and treatment of cancer for decades. However, the increasing number of new cases of cancer and the high mortality rate still pose a huge challenge to the current clinical cancer treatment methods. Existing mainstream cancer treatments include surgical resection, chemotherapy, or radiation therapy, but these treatments have their own limitations. Although surgical resection has a good therapeutic effect on early-stage solid tumors, its therapeutic effect on metastatic tumors is limited. In addition, in order to ensure the curative effect during the operation, a large amount of normal tissue adjacent to the tumor is often removed, thereby causing significant damage to the patient's body. Chemotherapy is a commonly used clinical treatment method to control tumor growth through systemic administration. While killing cancer cells, it also kills a large number of normal cells, and it is easy to induce cancer cells to develop resistance to chemotherapeutic drugs, which often leads to the failure of treatment [12].

Radiation therapy is a common clinical cancer treatment method that induces cancer cell death by irradiating cancer cells with radionuclides or ionizing radiation. Due to the controllability of radiation, that is, the irradiation range, the systemic toxicity caused by radiotherapy is significantly lower than that of chemotherapy by systemic administration. However, radiotherapy still irradiates the normal tissues around the tumor to different degrees, causing obvious side effects. In view of this, on the basis of existing cancer treatment methods, combined with the advantages of multiple disciplines such as tumor biology, material science, and instrument manufacturing, new cancer treatments are developed. It has received more and more attention and research to meet the needs of current clinical cancer patients.

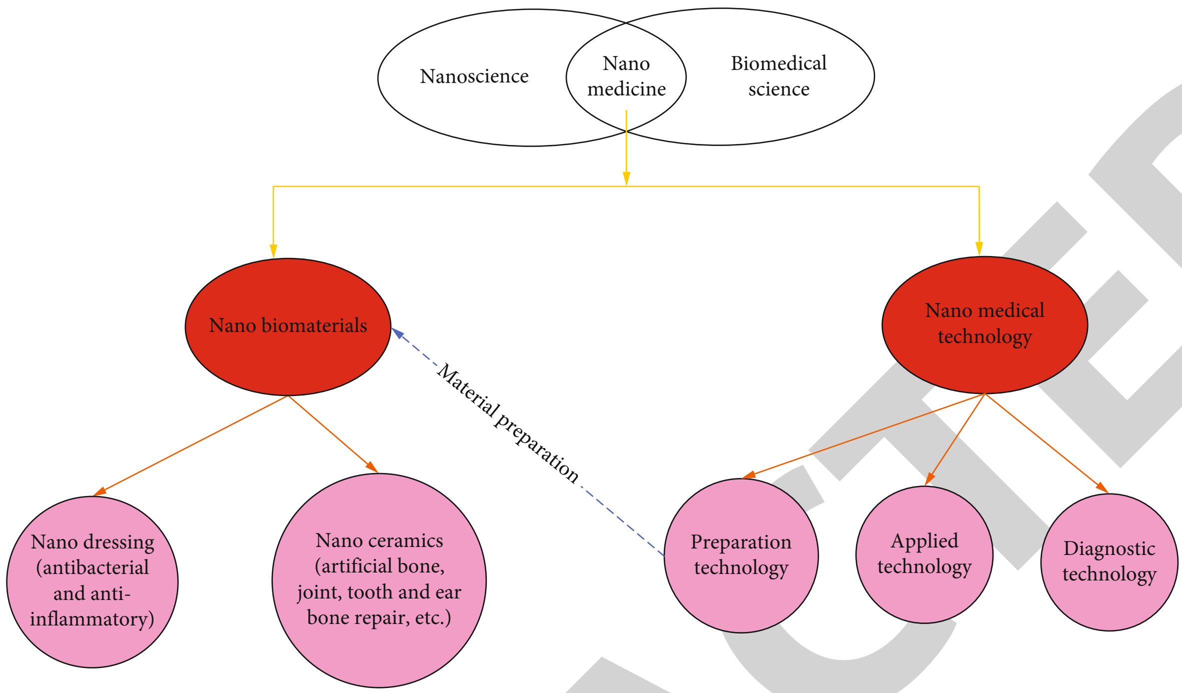

Figure 2: Overview of nanomedicine.

At present, a large number of studies have shown that many new cancer treatment methods (such as tumor immunotherapy, phototherapy, and gene therapy) and tumor treatment strategies under image navigation have good application prospects. At the same time, by combining with the commonly used clinical treatment methods, it also endows these traditional cancer treatment methods with new vitality and development opportunities and provides new options for the safe and efficient treatment of tumors [13].

3.2. Application of Nanomaterials. In the past few decades, nanomaterials have been extensively researched and developed and have been successfully applied in the fields of catalysis, medicine, sensors, and biology. In particular, it has also received extensive attention in water treatment and wastewater treatment. Moreover, the flow properties of nanomaterials in solution are very high. Nanomaterials have a relatively large specific surface area due to their small size, so they have strong adsorption capacity and reactivity. It has been reported that heavy metals, organic pollutants, inorganic anions, and bacteria can be successfully removed by many kinds of nanomaterials [14].

Due to the unique size-dependent properties of nanomaterials, they have a profound impact on various application fields such as the construction industry, products of daily life, and medical and healthcare. Figure 2 is an overview of nanomedicine.

Nano-antibacterial materials have attracted much attention due to their stable performance, good antibacterial effect, and low price. For example, nanotitanium oxide material has photocatalytic effect, which can decompose toxic gases such as formaldehyde and benzene and kill bacteria on its surface. Nanometer self-cleaning materials have great development space. Nanomaterials also have many applications in catalysis. Catalysts play an important role in the field of chemistry. Catalysts can increase the reaction rate and shorten the reaction time. Most of the traditional catalysts have low catalytic efficiency and difficult preparation, resulting in waste of raw materials, reducing economic benefits, and polluting the environment. Nanomaterials have many active sites. It can greatly improve the reaction rate and control the progress of the reaction. It can even make chemical reactions that were previously inoperable go smoothly.

Nanoparticles used as catalysts are as follows:

(1) Metal nanoparticles

(2) Nanoparticles are supported on porous supports, which can further increase the selectivity of catalysts

(3) Compound nanoparticles

Nanomaterials are used in lithium electrical energy to improve cycle life. It can undergo some reactions that cannot occur in other materials, increasing the charge-discharge rate [15]. At present, nanomaterials can be well used as contrast agents in medical imaging. The mechanism by which nanobiomaterials promote the repair of damaged tissue is shown in Figure 3. Nanoparticles are widely used in biomedicine and can be used as biochips, bioprobes, etc. New medicines require new means of drug delivery so that side effects can be reduced and better efficacy can be achieved. Nanotechnology drug delivery can deliver drugs directly to cells and to targeted tissues.

3.3. Unsupervised Learning. The difference between unsupervised learning and supervised learning is that data does

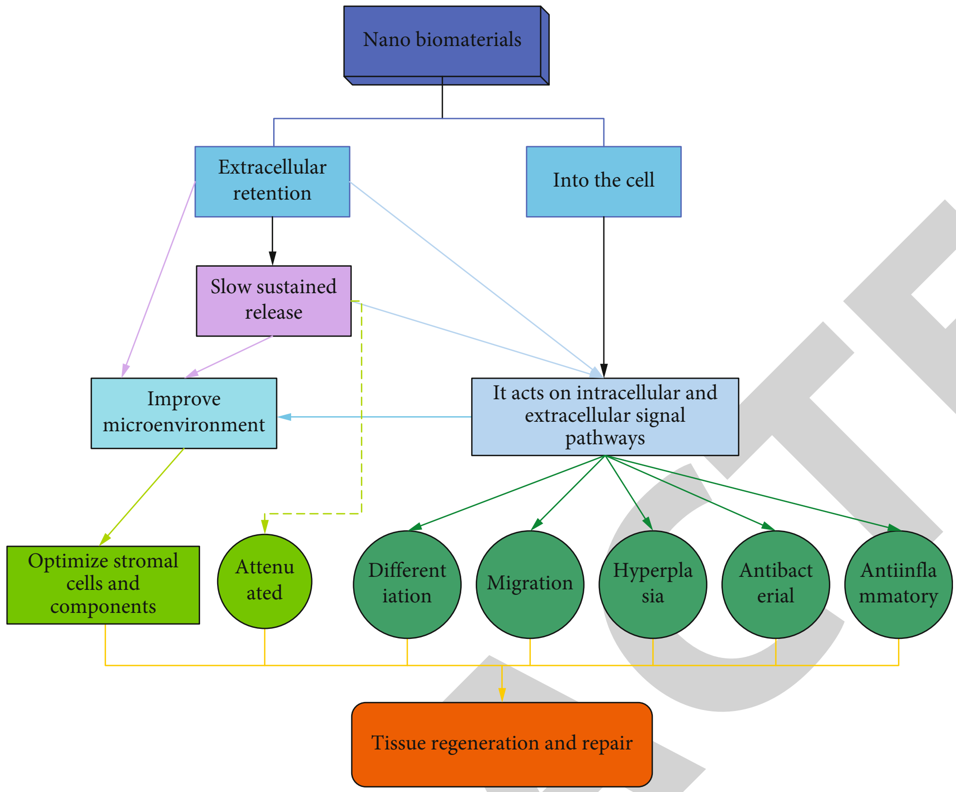

FIGURE 3: Mechanism of nanobiomaterials to promote repair of damaged tissue.

not need to be identified in advance. According to different learning method rules and the clustering characteristics of the data itself, this paper finds the corresponding internal rules and finds useful hidden information in the complex and disordered data [16].

3.3.1. Clustering Algorithm. Clustering algorithm is a kind of classification and grouping of things with the same attributes. It classifies cluttered sets of data into meaningful clusters. The essence of a clustering problem is an optimization problem, but this optimization must satisfy certain clustering conditions or clustering rules. The advantage of clustering is that the processing time is fast, the operation is simple, and it is easy to explain; the disadvantage is that the parameters need to be set when using, and sometimes, the result may be locally optimal. The classification of clustering algorithms is shown in Figure 4 [17, 18].

(1) Data Standardization. In order to eliminate the influence of different dimensions of the original data, this paper adopts the cluster analysis method in the data preprocessing, and the original data needs to be standardized. The normalized formula is

$$A_{mn} = \frac{B_{mn} - \overline{B_n}}{\sqrt{\text{var}\ (B_n)}} \quad (m = 1, 2, \cdots, j), \tag{1}$$

$$\overline{B_n} = \frac{1}{j} = \sum_{m=1}^{j} B_{mn}, \tag{2}$$

$$\sqrt{\text{var}\ (B_n)} = \sqrt{\frac{1}{j}\sum_{m=1}^{j} (B_{mn} - B_n)^2}, \tag{3}$$

(2) Define the Distance. Assuming that there are j sample data in a b-dimensional space, the formula for calculating the distance between sample m and sample n is as follows:

$$D_{mn} = \sum_{k-1}^{b} |A_{mk} - A_{nk}|. \tag{4}$$

The formula calculates the absolute value distance.

$$D_{mn} = \sqrt{\sum_{k=1}^{b} (A_{nk} - A_{mk})^2}. \tag{5}$$

The formula calculates the Euclidean distance.

$$D_{mn} = \text{MAX}_{1 \le k \le b} |A_{mk} - A_{nk}|. \tag{6}$$

The formula calculates the Chebyshev distance.

Usually, the smaller the distance is, the closer the similarity of the sample objects of the study is.

(3) Similarity Coefficient. The similarity coefficient of any two b-dimensional vectors can be used to measure the similarity of these two vectors in the b-dimensional space. The

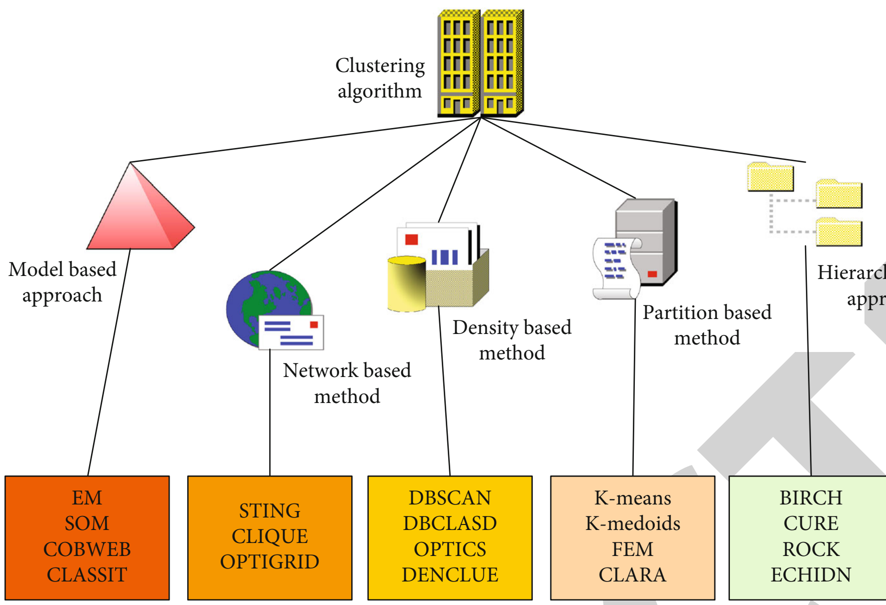

Figure 4: Classification of clustering algorithms.

similarity coefficient C_{mn} is used to represent, where m and n are the two vectors to be compared. C_{mn} satisfies symmetry; that is, the two vectors to be compared satisfy $C_{mn} = C_{nm}$. In general, the cosine of the angle between two vectors is a common similarity coefficient:

$$\mathrm{COS}(\theta_{mn}) = \frac{\sum_{k=1}^{b} A_{mk}A_{nk}}{\sqrt{\sum_{k=1}^{b} A_{mn}^2 A_{nk}^2}}. \quad (7)$$

3.3.2. K-Means Clustering

(1) K-Means Algorithm. The K-means algorithm is an unsupervised algorithm. As a classical clustering method, it is widely used to solve various partitioning and clustering problems, and it is still one of the most widely used clustering algorithms. At the same time, the K-means algorithm is also the basis for many more complex clustering techniques. While there have been many improvements to clustering methods today, the K-means algorithm is not outdated or obsolete and, in fact, may be more popular now than ever. The central idea of K-means clustering is to divide n data objects according to the number of categories K given in advance, so as to minimize the difference within each class and maximize the difference between classes. The flowchart of the K-means algorithm is shown in Figure 5 [19, 20].

The K-means algorithm is also known as the k-means algorithm. The algorithm idea is roughly as follows: it randomly selects k samples from the sample set as cluster centers and calculates the distances between all samples and the k "cluster centers." For each sample, it is divided into the cluster where the closest "cluster center" is located, and the new "cluster center" of each cluster is calculated for the new cluster.

According to the description, we can roughly guess the three main points for implementing the K-means algorithm: selection of the number of clusters k, the distance from each sample point to the "cluster center", and according to the newly divided cluster, updating the "cluster center."

(2) Key Points of K-Means Algorithm.

(1) Selection of k value

The choice of k is generally determined according to actual needs, or the value of k is directly given when the algorithm is implemented.

(2) The measure of distance

A sample is given:

$$M^i = \left\{M_1^i, M_2^i, \cdots, M_p^i\right\}, \quad (8)$$

$$M^j = \left\{M_1^j, M_2^j, \cdots, M_p^j\right\}, \quad (9)$$

where $i, j = 1, 2, \cdots, t$ represents the number of samples and p represents the number of features.

(a) Ordinal attribute distance measures (discrete attributes {1, 2, 3} or continuous attributes)

Minkowski distance

$$D_{\mathrm{mk}}\left(M^{(i)}, M^{(j)}\right) = \left(\sum_{u=1}^{p} \left|M_u^i - M_u^j\right|^h\right)^{1/h}. \quad (10)$$

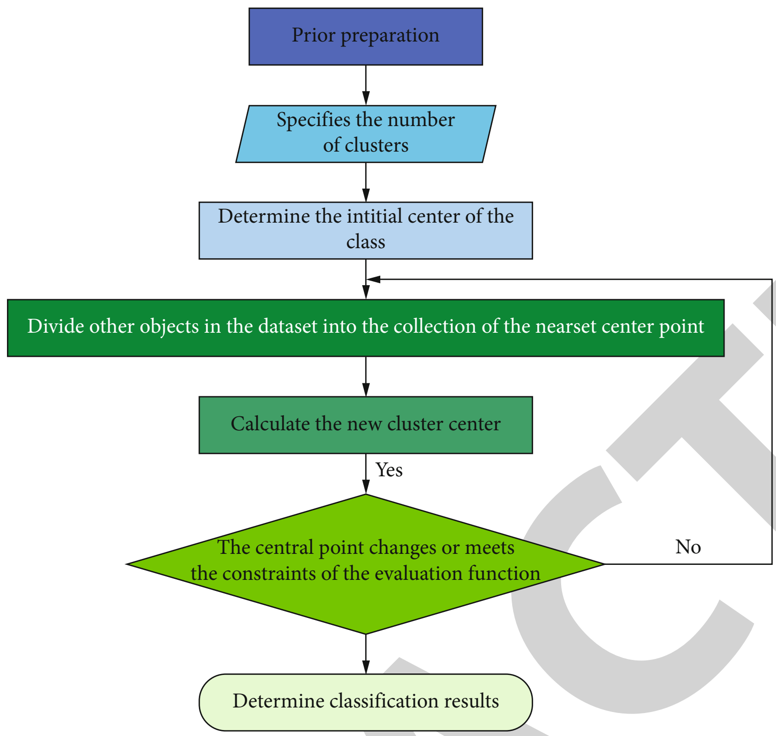

Figure 5: Flowchart of the classic K-means algorithm.

Euclidean distance refers to the Minkowski distance when $h = 2$:

$$D_{\mathrm{ed}}\left(M^{(i)}, M^{(j)}\right) = \left\|M^{(i)} - M^{(j)}\right\|_2 = \sqrt{\sum_{u=1}^{p} \left|M_u^i - M_u^j\right|^2}. \quad (11)$$

Manhattan distance refers to the Minkowski distance when$h = 1$:

$$D_{\mathrm{man}}\left(M^{(i)}, M^{(j)}\right) = \left\|M^{(i)} - M^{(j)}\right\|_1 = \sum_{u=1}^{p} \left|M_u^i - M_u^j\right|. \quad (12)$$

(b) Disordered attribute distance metrics (such as {airplane, train, ship})

VDM (Value Difference Metric)

$$\mathrm{VDM}_h\left(M_u^i, M_u^j\right) = \sum_{g}^{k} \left|\frac{y_u, M_u^i, g}{y_u, M_u^i} - \frac{y_u, M_u^j, g}{y_u, M_u^j}\right|^h. \quad (13)$$

Among them, y_u, M_u^i represents the number of samples whose value is M_u^i on attribute u, and y_u, M_u^i, g represents the number of samples whose value is M_u^i on attribute u in the g th sample cluster. $\mathrm{VDM}_h(M_u^i, M_u^j)$ represents the VDM distance between two discrete values M_u^i and M_u^j on attribute u.

(c) Mixed attribute distance metric, which is a combination of ordered and disordered:

$$\mathrm{MinkovDM}_h\left(M^i, M^j\right) = \left(\sum_{u=1}^{p_s} \left|M_u^i - M_u^j\right|^h - \sum_{u=p_s+1}^{p} \mathrm{VDM}_h\left(M_u^i, M_u^j\right)\right)^{1/h} \quad (14)$$

Among them, p_s contains ordered attributes and $p - p_s$ unordered attributes.

The data set in this article is a continuous attribute, so the Euclidean distance is mainly used in the code to measure the distance.

(3) Update "cluster center"

For each divided cluster, calculate the mean value of the sample points in each cluster, and it uses the mean value as the new cluster center.

3.4. Genetic Algorithms

3.4.1. Overview. Genetic algorithm (GA) is a new global optimization algorithm developed in recent years. It is based on evolution theory and adopts design methods such as genetic combinatorial optimization technology, genetic variation, and natural selection.

Genetic algorithm is an optimization search algorithm based on biological evolution theory and molecular genetics. It first encodes possible solutions to a particular problem, called chromosome-encoded solutions. This paper randomly selects N chromosomes as the initial group and then calculates the fitness of each chromosome according to the value of the evaluation function. It is predetermined that the best performance value of a chromosome is the highest fitness value, the chromosome with the highest fitness value is selected for replication, and a new set of chromosomes is created. These chromosomes are more customized to the environment through genetic operators. People will eventually adapt to the new environment, and forming a better group becomes the best solution to the problem [21, 22].

3.4.2. Basic Algorithm. The execution of the genetic algorithm involves many random operations, first considering the result of the selection. In standard genetic algorithms, selection criteria are based on the principle of proportionality. Therefore, through the action of the ith selector, the expected value of the number of people who will continue to exist in the next generation is $n(g_i/\sum g)$; then, there is

$$\bar{g}(P,t) = \frac{1}{n(P,t)} \sum g_i. \tag{15}$$

Then,

$$n(P,t+1) = n(P,t) \cdot \frac{\bar{g}(P,t)}{g(t)}. \tag{16}$$

The equation shows that the effect of the selection operator will increase (decrease) the ability of a pattern above (below) the average to be applied across generations, improving quality.

Then, it analyzes the role of the crossover operator. This plan can obviously be maintained in the next generation if there is no intersection or if the intersection point is beyond the character positions specified on the left and right ends of the figure. Therefore, the probability R_s that the P mode will continue to exist in the next generation should satisfy

$$R_s \geq 1 - R_c \cdot \frac{\varphi(P)}{(L-1)}. \tag{17}$$

Taking into account the effects of selection and crossover, there are

$$n(P,t+1) \geq n(P,t) \cdot \bar{f}(P,t) \cdot \left[\frac{1 - R_c \cdot \varphi(P)}{(L-1)/\bar{g}(t)}\right]. \tag{18}$$

Finally, because R_m represents the probability of the mutation operator acting, the constant probability is $1 - R_m$. If all the specified characters remain unchanged, the P pattern can naturally continue to exist in the next generation, the probability $(1-R_m)^{O(P)}$; R_m is usually not large; then, under the action of the mutation operator, the probability of P continuing to exist is

$$(1-R_m)^{O(P)} \approx 1 - R_m \cdot O(P). \tag{19}$$

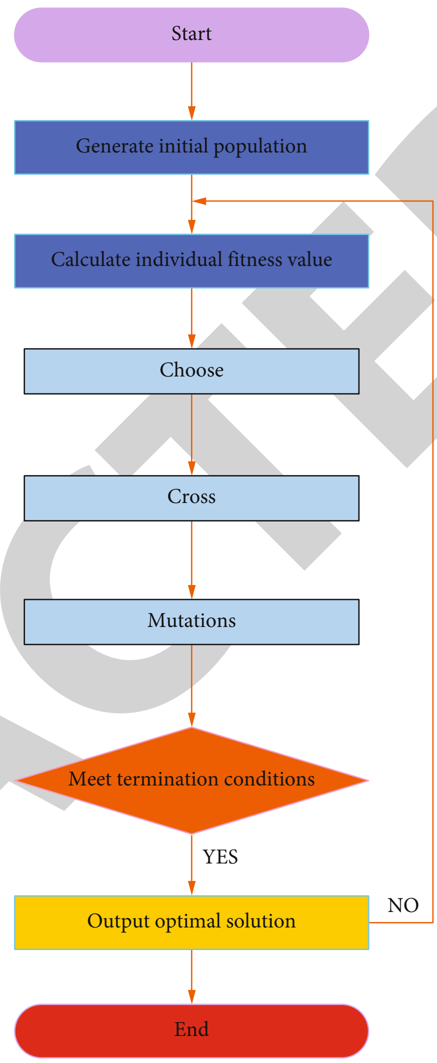

Figure 6: Genetic algorithm flowchart.

The probability of unreserved is about $O(P) \cdot R_m$. So, taking into account the functions of selection, crossover, and mutation operators, we end up with

$$n(P,t+1) \geq n(P,t) \cdot \bar{g}(P,t) \cdot \frac{[1 - R_c \cdot (\varphi(P)/(L-1)) \cdot R_m]}{\bar{g}(t)}. \tag{20}$$

Specifically, if $\bar{g}(P,t) = g(t)(1+c)$, $c > 0$ is a constant, then

$$n(P,t) = n(P,t-1)(1+c) = n(P,O)(1+c)^t. \tag{21}$$

The flowchart of the standard genetic algorithm is shown in Figure 6.

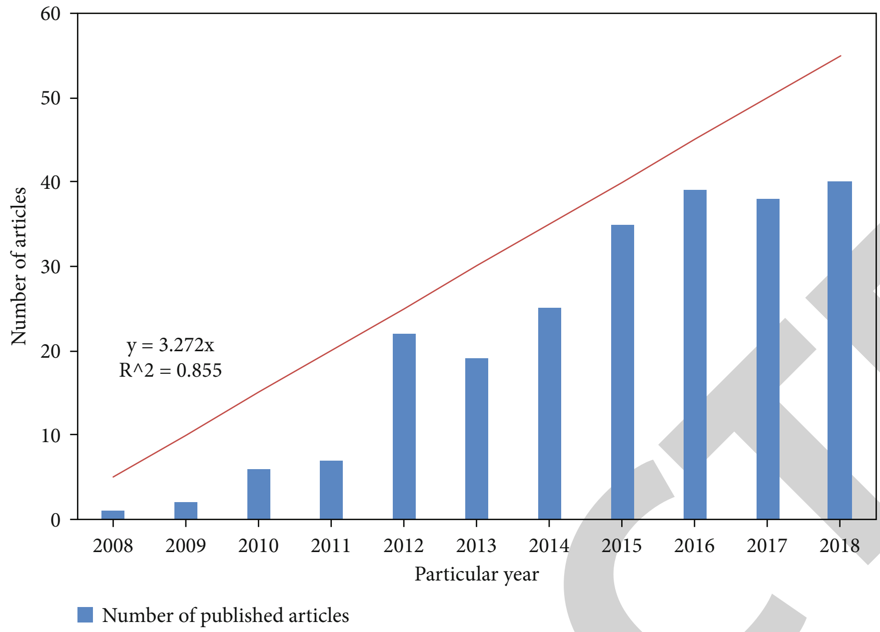

FIGURE 7: 2008-2018 published status of systematic review and meta-analysis of traditional Chinese medicine injections in the treatment of tumor diseases at home and abroad.

4. Network Meta-Analysis Experiment of Traditional Chinese Medicine Injections in the Treatment of Digestive System Tumors

4.1. Current Status of Systematic Review/Meta-Analysis of Traditional Chinese Medicine Injections in the Treatment of Tumor Diseases. Since the publication of the first systematic review of TCM injections for oncology in 2008, with the increase of years, the number of publications of related systematic reviews/meta-analyses has also increased ($y = 3.272x$, $R^2 = 0.855$). As shown in Figure 7 3 papers were published before 2009, 35 papers were published from 2010 to 2012, 156 papers were published from 2013 to 2017, and 40 papers were published in 2018 [23].

4.2. Tumor Types Involved. Among the 198 systematic reviews/meta-analyses retrieved, 2 classic meta-analyses are aimed at the treatment of multiple tumors with a single variety of traditional Chinese medicine injections. In addition, the other 196 such systematic reviews/meta-analyses were all single-species or multispecies TCM injections for the treatment of a single type of tumor. The total frequency of occurrence of different types of tumors was 200. Among them, non-small-cell lung cancer has the most evaluation times, with 77 evaluation times, accounting for 38.5% of the total frequency of tumor types. This may be related to the fact that lung cancer ranks first in the morbidity and mortality of malignant tumors. The second was the evaluation times of liver cancer and gastric cancer, which were 29 and 25, respectively, accounting for 14.5% and 12.5% of the total frequency of tumor types. In addition, 17 studies only mentioned evaluating the disease as "tumor." It does not describe the type of tumor in detail. The types of tumors involved are shown in Table 1. The number of cases for different types of tumors is shown in Figure 8.

4.3. Involving Varieties of Traditional Chinese Medicine Injections. Among the 198 systematic reviews/meta-analyses included in this study, 14 network meta-analyses and 4 classic meta-analyses, respectively, evaluated multiple varieties of traditional Chinese medicine injections. The rest of the literature is only for a single variety of traditional Chinese medicine injections. A total of 14 TCM injection varieties were involved in the included systematic review/meta-analysis. The total occurrence frequency of different varieties of traditional Chinese medicine injections is 352 times. It accounted for 15.6% of the total frequency of Chinese medicine injections, followed by Shenqi Fuzheng injection and Aidi injection; the frequency of occurrence was 50 times and 45 times, accounting for 14.2% and 12.8%, respectively. For traditional Chinese medicine injections, there is a frequency of 10 or more occurrences, as shown in Table 2, for the varieties involved in the evaluation. It includes Fufang Kushen injection, Shenqi Fuzheng injection, Aidi injection, Kangai injection, Cinobufasu injection, Kanglaite injection, Brucea oil emulsion injection, Xiaoaiping injection, and Delisheng injection.

At the same time, this study summarizes the following 14 varieties of traditional Chinese medicine injection components and functional indications. It further analyzes the relationship between its components, efficacy and indications, and the treatment of tumors.

A summary of the dominant varieties of traditional Chinese medicine injections based on cluster analysis is shown in Table 3.

(1) To carry out the evaluation of clinical efficacy of traditional Chinese medicine injections in the treatment of gastric cancer, esophageal cancer, liver cancer, bowel cancer, and pancreatic cancer using network meta-analysis and the ranking of the

Table 1: Statistics of tumor types involved.

Serial number	Disease	Frequency of occurrence	Percentage
1	Non-small-cell lung cancer	77	38.5%
2	Liver cancer	29	14.5%
3	Gastric cancer	25	12.5%
4	Tumor	17	8.5%
5	Malignant pleural and peritoneal effusion	12	6%
6	Colorectal cancer	9	4.5%
7	Lung cancer	8	4%
8	Mammary cancer	8	4%
9	Esophageal cancer	8	4%
10	Cancer pain	4	2%
11	Lymphoma	3	1.5%

therapeutic effects. The ranking of different outcome indicators suggests that traditional Chinese medicine injections are the best drugs for the treatment of different digestive system tumors. The cluster analysis results show that (1) for the treatment of gastric cancer with traditional Chinese medicine injection combined with FOLFOX chemotherapy, in terms of improving the total clinical efficiency and improving the quality of life, astragalus polysaccharide combined with FOLFOX chemotherapy and Kangai injection combined with FOLFOX chemotherapy have more advantages than other traditional Chinese medicine injections. In terms of alleviating adverse reactions, astragalus polysaccharide combined with FOLFOX chemotherapy, sodium cantharidate, and vitamin B and FOLFOX chemotherapy have advantages over other traditional Chinese medicine injections. In addition, in the treatment of gastric cancer with traditional Chinese medicine injection combined with XELOX chemotherapy, Brucea chinensis oil emulsion and compound Sophora flavescens have more advantages than other traditional Chinese medicine injections in improving the total clinical effective rate and improving the quality of life indicators. Mushroom polysaccharide has more advantages than other traditional Chinese medicine injections in terms of alleviating adverse reaction indicators. (2) In improving the survival rate of patients with esophageal cancer, cinobufacini and Kangai injections combined with radiotherapy are dominant in the comprehensive ranking. Compound Sophora flavescens injection combined with radiotherapy has an advantage in the comprehensive ranking of the clinical total effective rate and the improvement of quality of life. (3) In the study of traditional Chinese medicine injection combined with hepatic artery embolization in the treatment of liver cancer, compared with the cluster analysis results of other traditional Chinese medicine injections, Brucea oil emulsion and cinobufagin combined with TACE were dominant in the comprehensive ranking of survival rate. Kanglaite and astragalus polysaccharide combined with TACE are dominant in the comprehensive ranking of clinical total effective rate and quality of life improvement. Shenmai combined with TACE is dominant in the comprehensive ranking of adverse reactions. (4) Compared with the cluster analysis results of other traditional Chinese medicine injections, Xiaoaiping injection assisted by FOLFOX chemotherapy regimen in the treatment of colorectal cancer has the advantage in the comprehensive ranking of clinical efficacy and quality of life improvement

(2) In terms of safety, traditional Chinese medicine injections combined with radiotherapy or chemotherapy can alleviate the occurrence of adverse reactions. However, few adverse reactions caused by TCM injections have been reported in RCTs, so no definite conclusion can be drawn

4.4. Establishment of Animal Tumor Model. The experimental animals were BALB\c mice, 4.4-6.5 weeks old, weighing 11-16 g, female. In large-scale culturing of murine breast cancer cells 4T1, collecting 4T1 cells in the logarithmic growth phase, and counting them in a cytometer, the medium was used to prepare a cell suspension of1×10^7 /mL. The $50 \mu L$ cell suspension was subcutaneously injected into the right back of BALB\c mice. After one week of culture, the tumor size was measured with a vernier caliper regularly. When the tumor volume was about $58 - 110 mm^3$, it could be used as a tumor model for in vivo research. Tumor volume was calculated according to the following formula:

$$V_{\text{Tumor volume}} = L_{\text{Tumor length diameter}} \cdot \frac{M^2_{\text{The widest diameter of a tumor perpendicular to the longest diameter}}}{2}. \quad (22)$$

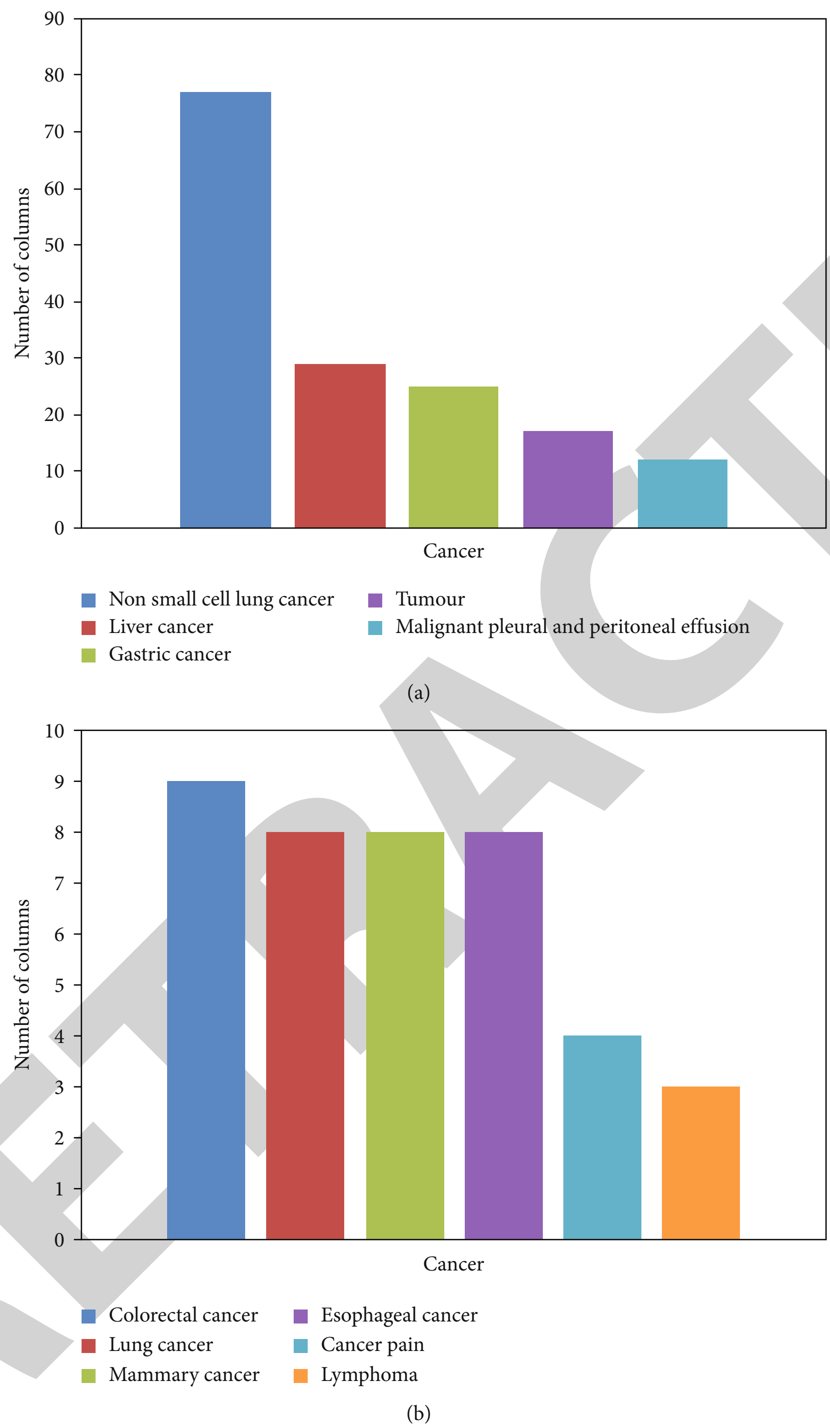

FIGURE 8: Plot of the number of cases for different types of tumors.

In order to observe the histopathological changes of SM-NPs in photothermal/photodynamic synergistic treatment of tumors, a single dose of PBS, free Ce6, and SM-NPs was injected into tumor-bearing mouse via tail vein. The tumor tissue was irradiated with laser 24 hours after administration, and a nonirradiated control group was set, respectively. Six hours after laser irradiation, the tumor-bearing mice were sacrificed and the heart, liver, spleen, lung, kidney, and tumor tissues were taken out for H&E staining. It can be seen from Table 4 that sporadic areas of cell necrosis and infiltration of inflammatory cells can be observed in the tumor tissue of the free Ce6 light treatment group. In the SM-NP tumor tissue, obvious necrosis area and a large number of inflammatory cell infiltration can be seen. The results showed that the therapeutic effect of the SM-NP light therapy group on tumor was significantly higher than that of

Table 2: Statistics of traditional Chinese medicine injection varieties involved in the systematic review/meta-analysis of tumor diseases.

Serial number	Disease	Frequency of occurrence	Percentage
1	Compound Sophora flavescens injection	55	15.6%
2	Shenqi Fuzheng injection	50	14.2%
3	Aidi injection	45	12.8%
4	Kangai injection	35	9.9%
5	Cinobufacini injection	29	8.2%
6	Kanglaite injection	27	7.7%
7	Javanica oil emulsion injection	25	7.1%
8	Xiaoaiping injection	18	5.1%
9	Delisheng injection	14	4.0%
10	Elemene injection	13	3.7%
11	Lentinan injection	12	3.4%
12	Ginseng polysaccharide injection	10	2.8%
13	Shenfu injection	10	2.8%
14	Astragalus polysaccharide injection	9	2.6%

Table 3: Summary table of dominant varieties of traditional Chinese medicine injection based on cluster analysis.

Name of digestive system tumor	Intervention measures of the control group	Outcome indicators	The dominant varieties of traditional Chinese medicine injection obtained by cluster analysis
Gastric cancer	FOLFOX chemotherapy regimen	Total clinical effective rate, quality of life, and adverse reactions	Astragalus polysaccharide injection, Kangai injection, sodium pincer, and vitamin B injection
Gastric cancer	XELOX chemotherapy regimen	Total clinical effective rate, quality of life, and adverse reactions	Brucea javanica oil emulsion injection, compound Sophora flavescens injection, Lentinan injection
Esophageal cancer	Radiotherapy	Clinical total effective rate, quality of life, adverse reactions, survival rate	Compound Sophora flavescens injection, Shenqi Fuzheng injection, compound Sophora flavescens injection, Cinobufagin injection, Kangai injection
Esophageal cancer	Chemotherapy	Total clinical effective rate, quality of life, and adverse reactions	Compound Sophora flavescens injection
Liver cancer	TACE	Clinical total effective rate, quality of life, adverse reactions, survival rate	Brucea javanica oil emulsion injection, cinobufagin injection, Kanglaite injection, astragalus polysaccharide injection, Shenmai injection
Colon cancer	FOLFOX chemotherapy regimen	Total clinical efficiency and quality of life	Xiaoaiping injection
Pancreatic cancer	Chemotherapy	Total clinical effective rate, quality of life, and adverse reactions	Javanica oil emulsion injection, Kanglaite injection, Aidi injection

the free Ce6 light therapy group, and its destruction and killing effect on the tumor tissue was greater. Table 4 shows that the histopathology of the heart, liver, spleen, lung, and kidney tissue in each treatment group has no obvious changes. The results showed that although SM-NPs had a strong killing effect on tumor tissue, it was safe for the heart, liver, spleen, lung, kidney, and other tissues and had no obvious toxic and side effects.

5. Discussion

At present, malignant tumor has become one of the most serious diseases threatening human health. The World Health Organization's report on cancer in the world says there are 14 million new cancer cases and 8.2 million deaths worldwide each year. When malignant tumors occur, it increases the difficulty of treatment and the risk of life. Therefore, how to effectively prevent and treat cancer, especially to prevent tumor metastasis or recurrence, is an urgent problem to be solved in current scientific research.

There are three main methods of treating cancer: surgery, chemotherapy, and radiation. However, traditional treatment methods have disadvantages such as large trauma, large toxic and side effects, prone to multidrug resistance, damage to the immune system, and difficulty in avoiding tumor recurrence. In recent years, tumor immunotherapy has become one of the important research fields, an important breakthrough, and an important development direction of tumor therapy.

Table 4: The ratio of tumor volume to the volume before treatment in each group after 12 days of treatment and the comparison results between each group (t test).

Project	SM-NPs/IR	SM-NPs/Vc/IR	Ce6/IR	PBS/IR	SM-NPs	Ce6
$\frac{V_{\text{After treatment}}}{V_{\text{Before treatment}}}$ $(\bar{X} \pm S)$	0.42 ± 0.29	1.88 ± 0.34	3.08 ± 0.44	3.90 ± 0.29	3.43 ± 0.36	4.13 ± 0.29
SM-NPs/IR	—	0.000	0.000	0.000	0.000	0.000
SM-NPs/Vc/IR	—	—	0.052	0.007	0.007	0.002
Ce6/IR	—	—	—	0.289	0.272	0.103
PBS/IR	—	—	—	—	0.829	0.688
SM-NPs	—	—	—	—	—	0.529
Ce6	—	—	—	—	—	—

Phototherapy is a new way of thinking in current cancer treatment research. It is also one of the hottest research areas in biomedical applications, which is fundamentally due to the advantages of phototherapy with high treatment accuracy, minimal tissue damage, and no drug resistance. At present, the common phototherapy reagents mainly have shortcomings such as low absorbance, poor water solubility, easy aggregation, easy quenching of fluorescence, and poor dark toxicity. In this paper, combining the performance advantages of organic semiconductor nanoparticles and photosensitizers, a series of high-performance organic nano-phototherapy agents were designed, and their applications in tumor phototherapy were initially explored.

6. Conclusion

Organic semiconductor nanomaterials are nanostructured materials. Due to its strong light absorption, stable light, high brightness, and good biocompatibility, it has been widely used in bioimaging, antibacterial, antitumor, gene therapy, and drug release in the past decade. In this study, a network meta-analysis of traditional Chinese medicine injections in the treatment of digestive system tumors was carried out, and the clinical efficacy and safety of different varieties of traditional Chinese medicine injections were systematically, scientifically, and comprehensively evaluated. At the same time, Bayesian theory was used to identify the dominant varieties of traditional Chinese medicine injections and to optimize the program of adjuvant radiotherapy and chemotherapy for the treatment of digestive system tumors. It provides high-quality evidence-based medical evidence for clinical use.

Data Availability

No data were used to support this study.

Conflicts of Interest

The authors declare that there is no conflict of interest with any financial organizations regarding the material reported in this manuscript.

Authors' Contributions

Ying Liu and Yanwei Li contributed equally to this work and should be considered co-first authors.

Acknowledgments

This study was supported by Project supported by Sichuan Provincial Department of Education and Sichuan Research Center for Coordinated Development of TCM Culture (2020WH059). This study was supported by Chengdu Federation of Social Sciences Planning Project (YN2120200432).

References

[1] M. Li, H. Ma, C. Shi et al., "A cyanine-based liposomal nanophotosensitizer for enhanced cancer chemo-photodynamic therapy," *Chemical Research in Chinese Universities*, vol. 37, no. 4, pp. 925–933, 2021.

[2] W. Pan, M. Shi, Y. Li, N. Li, and B. Tang, "A GSH-responsive nanophotosensitizer for efficient photodynamic therapy," *RSC Advances*, vol. 8, no. 74, pp. 42374–42379, 2018.

[3] T. Akbari, M. Pourhajibagher, F. Hosseini et al., "The effect of indocyanine green loaded on a novel nano-graphene oxide for high performance of photodynamic therapy against _Enterococcus faecalis_," *Photodiagnosis & Photodynamic Therapy*, vol. 20, pp. 148–153, 2017.

[4] Y. Qin, B. Cao, J. Li, S. Liao, and X. Yu, "An oxygen-enriched photodynamic nanospray for postsurgical tumor regression," *ACS Biomaterials Science and Engineering*, vol. 6, no. 11, pp. 6415–6423, 2020.

[5] X. Zhang, J. Tang, C. Li, Y. Lu, and J. A. Liu, "A targeting black phosphorus nanoparticle based immune cells nano-regulator for photodynamic/photothermal and photo-immunotherapy," *Bioactive Materials*, vol. 6, no. 2, pp. 472–489, 2021.

[6] Y. Wang, M. Zu, X. Ma, D. Jia, and Z. Xu, "Glutathione-responsive multifunctional "Trojan Horse" nanogel as a nanotheranostic for combined chemotherapy and photodynamic anticancer therapy," *ACS Applied Materials & Interfaces*, vol. 12, no. 45, pp. 50896–50908, 2020.

[7] W. Deng, K. J. Mckelvey, A. Guller, A. Fayzullin, and E. M. Goldys, "Application of mitochondrially targeted nanoconstructs to neoadjuvant X-ray-induced photodynamic therapy for rectal cancer," *ACS Central Science*, vol. 6, no. 5, pp. 715–726, 2020.

[8] A. Mironov, K. A. Zhdanova, and A. B. Natal'ya, "Nanosized vehicles for delivery of photosensitizers in photodynamic diagnosis and therapy of cancer," *Chemistry*, vol. 87, no. 9, pp. 859–881, 2018.

[9] M. Overchuk, M. Cheng, and G. Zheng, "X-ray-activatable photodynamic nanoconstructs," *ACS Central Science*, vol. 6, no. 5, pp. 613–615, 2020.

[10] D. Cui, J. Huang, X. Zhen, J. Li, Y. Jiang, and K. Pu, "A semiconducting polymer nano-prodrug for hypoxia-activated photodynamic cancer therapy," *Angewandte Chemie International Edition*, vol. 58, no. 18, pp. 5920–5924, 2019.

[11] A. Oudin, J. Chauvin, L. Gibot et al., "Amphiphilic polymers based on polyoxazoline as relevant nanovectors for photodynamic therapy," *Journal of Materials Chemistry B*, vol. 7, no. 32, pp. 4973–4982, 2019.

[12] F. Ghorbani, A. Imanparast, F. Hataminia, and A. Sazgarnia, "A novel nano-superparamagnetic agent for photodynamic and photothermal therapies: an in-vitro study," *Photodiagnosis and Photodynamic Therapy*, vol. 23, pp. 314–324, 2018.

[13] K. Khatereh, R. Hosseinzadeh, and F. K. Shahidi, "Photodynamic treatment with anionic nanoclays containing curcumin on human triple-negative breast cancer cells: cellular and biochemical studies," *Journal of Cellular Biochemistry*, vol. 120, no. 4, pp. 4998–5009, 2019.

[14] W. Sun, T. Shi, L. Luo et al., "Monodisperse and uniform mesoporous silicate nanosensitizers achieve low-dose X-ray-induced deep-penetrating photodynamic therapy," *Advanced Materials*, vol. 31, no. 16, p. 1808024, 2019.

[15] W. Sijia, H. Liu, J. Xin et al., "Chlorin-based photoactivable galectin-3-inhibitor nanoliposome for enhanced photodynamic therapy and NK cell-related immunity in melanoma," *ACS Applied Materials & Interfaces*, vol. 11, no. 45, pp. 41829–41841, 2019.

[16] Y. I. Jeong, B. Cha, H. L. Lee et al., "Simple nanophotosensitizer fabrication using water-soluble chitosan for photodynamic therapy in gastrointestinal cancer cells," *International Journal of Pharmaceutics*, vol. 532, no. 1, pp. 194–203, 2017.

[17] M. Hu, Y. Zhong, S. Xie, H. Lv, and Z. Lv, "Fuzzy system based medical image processing for brain disease prediction," *Frontiers in Neuroscience*, vol. 15, 2021.

[18] A. L. Lin, S. Z. Li, and C. H. Xu, "A pH-responsive stellate mesoporous silica based nanophotosensitizer for in vivo cancer diagnosis and targeted photodynamic therapy," *Biomaterials Science*, vol. 7, no. 1, pp. 211–219, 2019.

[19] D. R. Kanniga, M. Gurusamy, and P. Vijayakumar, "An efficient cloud data center allocation to the source of requests," *Journal of Organizational and End User Computing*, vol. 32, no. 3, pp. 23–36, 2020.

[20] K. Zhang, X. Meng, Y. Cao et al., "Metal-organic framework nanoshuttle for synergistic photodynamic and low-temperature photothermal therapy," *Advanced Functional Materials*, vol. 28, no. 42, 2018.

[21] T.-Y. Kim, S.-H. Kim, and H. Ko, "Design and implementation of BCI-based intelligent upper limb rehabilitation robot system," *ACM Transactions on Internet Technology*, vol. 21, no. 3, pp. 1–17, 2021.

[22] H. Yavari, N. Ghasemi, B. Divband, Y. Rezaei, G. Jabbari, and S. Payahoo, "The effect of photodynamic therapy and polymer solution containing nano-particles of Ag /ZnO on push-out bond strength of the sealers AH-Plus and MTA Fillapex," *Dentistry*, vol. 9, no. 9, pp. e1109–e 1114, 2017.

[23] A. Teerakapong, T. Damrongrungruang, S. Sattayut, N. P. Morales, A. Sangpanya, and M. Tanapoomchai, "Fungicidal effect of combined nano TiO_2 with erythrosine for mediated photodynamic therapy on Candida albicans: an in vitro study," *Lasers in Dental Science*, vol. 1, no. 2-4, pp. 101–106, 2017.